Journal of Applied Polymer Science

Synergistic Effects of *N*, *N*′-bis (benzoyl) Sebacic Acid Dihydrazide and Talc on the Physical and Mechanical Behaviors of Poly(L-latic acid)

Hongqin Xiao, Dan Guo, Jianjun Bao

State Key Laboratory of Polymer Materials Engineering, Polymer Research Institute of Sichuan University, Chengdu 610065, China

Correspondence to: J. Bao (E-mail: jjbao2000@sina.com)

ABSTRACT: The important practical problem of poor heat stability of poly(L-lactic acid) (PLLA) is addressed by the addition of *N*, *N*′-bis (benzoyl) sebacic acid dihydrazide (BSAD) and talc as a nucleating agent system. The idea of incorporating talc into the PLLA/BSAD composites is that talc can provide supplementary nucleation effect with very small amount of BSAD (0.2 wt %) and therefore can improve the heat deflection resistance of PLLA materials. Effects of BSAD/talc on morphology, crystallization behavior, heat resistance, and mechanical properties of PLLA/BSAD/talc were investigated after annealing processes. The results indicated that the BSAD/talc system increased the crystallinity from 6.0% of pure PLLA to a maximum 42.9% by the synergistic effects of BSAD and talc increasing the growth of spherulites and nucleation density, respectively. After annealing at different temperatures, the heat deflection temperature (HDT) of PLLA was improved dramatically due to synergistic effects of BSAD/talc between restricted chain movement and acceleration of crystallization. At high temperature (above T_g), the thermo-mechanical properties of PLLA is mainly determined by the crystallinity and the reinforcement effect of talc acted as a filler. Moreover, effects of BSAD/talc on mechanical properties were discussed. © 2014 Wiley Periodicals, Inc. J. Appl. Polym. Sci. **2015**, *132*, 41454.

KEYWORDS: crystallization; nucleic acids; thermal properties

Received 18 April 2014; accepted 25 August 2014

DOI: 10.1002/app.41454

INTRODUCTION

Poly(L-lactic acid) (PLLA) derived from renewable resources is attracting lots of interest and publicity because of excellent biodegradability, relatively good biocompatibility and processability by conventional methods.[1] However, the application of PLLA tends to be limited in low impact strength and especially in poor heat resistance at high temperature. Under a flexural load of 455 kPa (using the protocol of ASTM 648), the heat deflection temperature (HDT) of PLLA is just about 55°C, so the poor heat resistance of PLLA prevents itself from being a practical replacement of non-renewable thermoplastic resin. Transparent or translucent PLLA products, for example, are very suitable to bottle, however, they make an obvious softening once the temperature of water is over 60°C.[2] Poor heat resistance of PLLA is due to its relatively low glass transition temperature (T_g) (about 50–60°C) and low crystallization rate. Generally, PLLA almost remains amorphous because of its limited orientation and high cooling rate in processes such as injection-molding. The aggregation structure of PLLA leads to its heat resistance depending on T_g and only PLLA crystalline phase can confer mechanical properties above T_g.[3,4] Therefore, it is essential for PLLA to raise the glass transition temperature or to improve the crystallinity.

In recent years, a number of methods, such as introducing crosslinking[6,7] and adding lactide derivatives and poly(D-lactide) (PDLA), have attracted much attention to improve heat stability of PLLA, however most of them have their own shortcomings. For example, Mitomo et al.[4] reported that once PLLA/(3%TAIC) was annealed at 90°C for 1 h, and then irradiated at 50 kGy, it showed typical heat stability above the glass transition temperature. However, the expensive irradiation apparatus and the strict requirements of PLLA, which must be thin plates, have limited the practical application.[8] By replacing the methyl group on the lactide ring with norbornene, cyclohexadiene, and isoprene substituents, Gina L. Fiore and coworkers generated a series of bicyclic and tricyclic lactide derivatives which can raise T_g of PLLA up to 119°C.[5] However, the application of this way encounters a bottleneck due to complicate preparation of lactide derivatives and strict reaction conditions. PDLA as an optical isomer of PLLA can form highly regular stereocomplex with PLLA resulted in increasing of crystallinity. The melting temperature of PLLA/PDLA was 40–50°C higher than pure PLLA and

HDT of PLLA increased from approximately 60°C to up to 190°C by physically blending with the polymer PDLA.[9–11] But smaller PDLA concentration has no obvious effects on decreased crystallization half-time.[3]

The common method to improve HDT of PLLA is annealing combined with adding nucleating agent. Researchers are screening various commercial and developmental nucleating agents and fillers for potential application in biopolymers.[12–15] Kawamoto et al. have investigated that benzoylhydrazide (BH) type compounds exhibited excellent improvement of crystallization of PLLA.[16,17] In particular, *N*, *N*′-bis (benzoyl) sebacic acid dihydrazide (BSAD) have been proved to be the most effective for acceleration of PLLA crystallization under high cooling rate of 50°C min^{-1}.[16] PLLA with 1 wt % BSAD exhibited very short crystallization half-time whose injection-molding cycle time was less than 3 min.[16] Because of its complicated preparation, it is inevitable for the high-cost of BSAD. Talc is a cheap and widely used extender which is able to nucleate the crystallization of polymers through an epitaxial mechanism.[18] In the case of PLLA, talc increases crystallization rate and the effect is related to talc concentration and crystallization temperature.[19] It is shown that the crystallization half-time of PLLA can be reduced by more than one order of magnitude to less than one minute when 1 wt % talc is added.[20]

This paper studied the effect of a minute dosage (only 0.2 wt %) of BSAD with high loading of talc on the crystallinity after annealing. The crystallinity and mechanical properties achieved in different conditions are compared using differential scanning calorimetry (DSC) and dynamic mechanical analysis (DMA). To evaluate the practicability of the nucleating agent system, PLLA produced by injection-molding following annealing were investigated by HDT, tensile, and notched impact tests. This information would be useful to develop better understanding of PLLA/BASD/talc composites and to manufacture PLLA products with higher heat resistance and better price advantage.

EXPERIMENTAL

Materials

Poly(L-lactic acid), (PLLA 2003D), comprising around 2% D-isomer, was purchased from NatureWorks LLC (USA), with the weight-average molecular weight (M_w) of 197 kDa and the density of 1.24 g/cm^3. BSAD, with melting point of 208°C, was supplied from Shanxi Institute of Chemical Industry (Shanxi, China). Talc, with size of 3000 mesh, was obtained from Guangxi longguang Talc Development (Guangxi, China).

Preparation of PLLA/BSAD/Talc Composites

After mixing PLLA, 0.2 wt % BSAD and talc (0 wt %, 4.7 wt %, 9.0 wt %, 13.0 wt %, 16.7 wt %) in a high-speed mixer (1000 rpm), the composites were prepared on TSSJ-25/40 co-rotating intermeshing twin-screw compounding extruder (Chenguang Plastics Machinery Research Institute, Chengdu, China) and named as PLLA-0.2-0, PLLA-0.2-4.7, PLLA-0.2-9.0, PLLA-0.2-13.0, PLLA-0.2-16.7, respectively. The PLLA and BSAD were dried at 85°C for 12 h in a vacuum oven before mixing. The standard splines for performance test were molded using an injection-molding machine (HAAKE Minijet, USA). For comparison, neat PLLA and PLLA with 4.7 wt % talc (PLLA-0-4.7) were subjected to the same extrusion and injection process to achieve thermal and stress histories identical to those of the composites.

Characterization

The dispersion of talc in the matrix was investigated by a Hitachi S-3400 (Japan) scanning electron microscope at a 10 kV accelerating voltage. The samples were frozen in liquid nitrogen and fractured. The fractured surfaces were coated with gold before investigation. DSC measurements of PLLA/BSAD/talc composite were taken on a NETZCH 204 Phoenix differential scanning calorimeter with sample weight 7–8 mg, using nitrogen as the purge gas. The sample was first heated from room temperature to 200°C at a heating rate of 10°C /min and kept molten at 200°C for 5 min, and then cooled down to 30°C at a cooling rate of 1°C /min to evaluate their ability to crystallize upon cooling. All the samples were annealed at 120°C for 5 min before test. The crystallinity of composite was calculated by eq. (1):

$$X_c(\%) = \frac{\Delta H_m - \Delta H_c}{\varnothing \Delta H_0} \times 100 \quad (1)$$

where $\varnothing$ is the weight fraction of PLLA matrix in the composites, ΔH_m is the measured endothermic enthalpy of melting, ΔH_c is the exothermic enthalpy that is absorbed by the crystals formed during heating, and ΔH_0 is the theoretical melting enthalpy of 100% crystalline PLLA which has a value of 93.7 J/g.[21] As for the calculation the value of melting enthalpy, the method of Analyze/Integrate Peak/Linear option in TA Universal Analysis was used to perform a peak integration using a linear baseline. A linear baseline is defined as a straight line drawn between the selected start and stop limits. To evaluate isothermal crystallization behaviors, the sample was heated from 25°C to 190°C at a heating rate of 20°C/min and maintained for 10 min. Subsequently, it was cooled rapidly at a cooling rate of 40°C/min to the isothermal temperatures of 100, 105, 110, 115, and 120°C, respectively, and then held at the isothermal temperature for 50 min, allowing crystallization.

The isothermal crystallization morphologies of pure PLLA and its composites were measured by a polarized optical microscopy (POM) (Leica Microsystem GmbH, Germany) with a hot-stage. Firstly, the sample placed between two glass slides was heated to melt completely and pressed to obtain a slice. Secondly, the sample was moved to the hot-stage with the setting temperature of 120°C and maintained at this temperature for 30 min. The crystallization morphologies of the samples were taken images via a digital camera.

DMA was performed in tensile mode on a DMAQ800 analyzer (USA) to evaluate the thermal-mechanical properties of samples. With a fixed frequency1 Hz, dynamic temperature scans were carried out at a heating rate of 3°C/min from 30°C to 140°C. HDT test was carried out on a HDV2 (ATLAS, USA) testing machine. The tensile testing was carried out at the rate of 50 mm/min according to ASTM D 638-08 on standard type samples using an INSTRON 5567 (USA) universal testing machine. Notched impact strength testing was performed on a

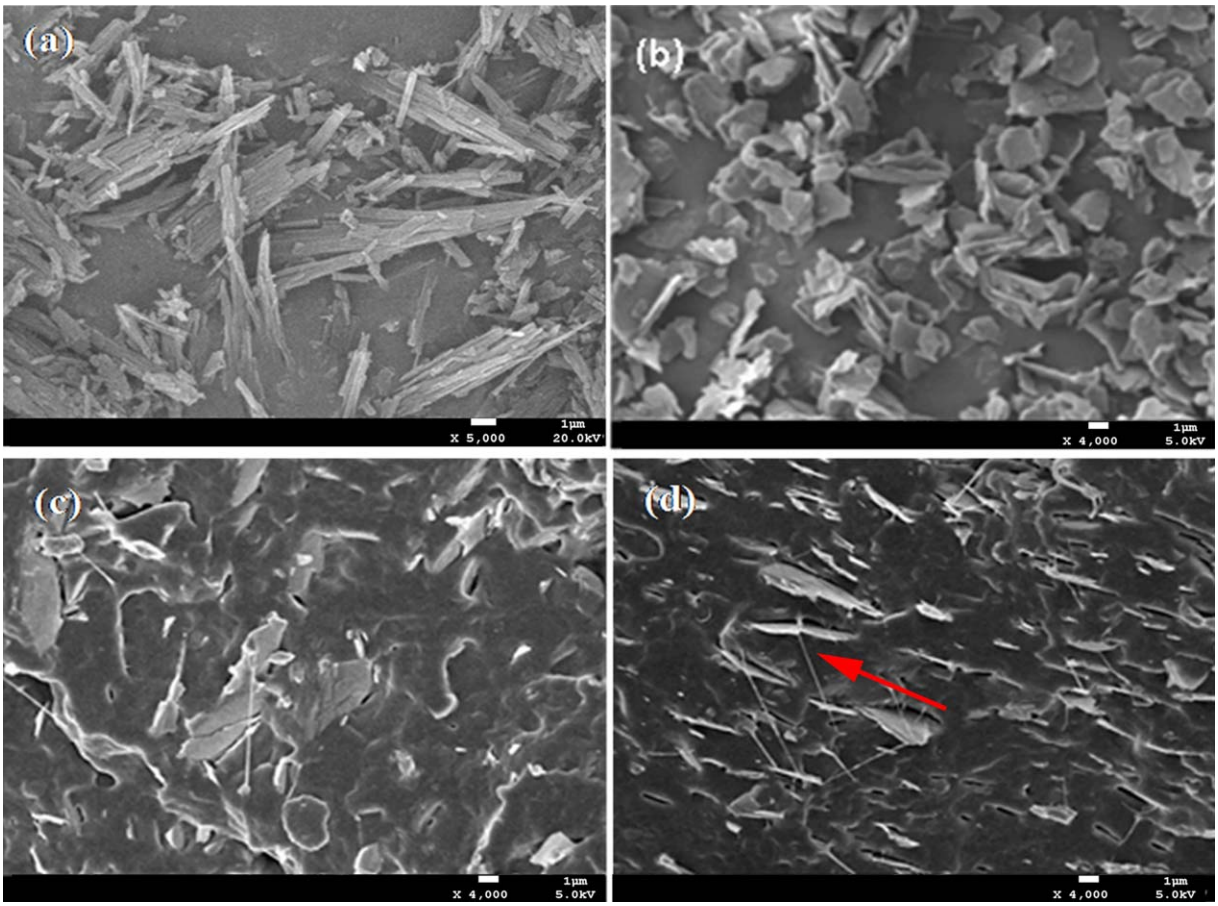

Figure 1. SEM micrographs of (a) BSAD, (b) talc, (c) PLLA-0.2–4.7, and (d) PLLA-0.2-16.7. [Color figure can be viewed in the online issue, which is available at wileyonlinelibrary.com.]

ZBC-4B Pendulum impact testing machine (Shenzhen Synopsys Measurement Ltd, China) according to ASTM D 256-06 at room temperature. All test specimens were annealed at 120°C for 5 min.[3,15]

RESULTS AND DISCUSSION

Morphology

Figure 1 shows the SEM image of (a) BSAD, (b) talc, (c) PLLA-0.2-4.7, and (d) PLLA-0.2-16.7. BSAD has been proved to be one of the most effective nucleating agents for PLLA. As seen from the Figure 1(a), the morphology of BSAD is needle-like or columnar with an excellent aspect ratio. In general, the nucleating agents with oriented shape,[22] such as fibrous, needle-like, columnar have an outstanding effect on nucleation. BSAD in particular is dissolved in PLLA matrix during melt mixing then precipitates and crystallizes before PLLA during cooling process, which can form numerous and well-distributed tiny needle-like crystallites in matrix. Because of the hydrogen bonding between the C═O group of PLLA and the N─H group of BSAD, these numerous tiny fibrous crystallites can significantly promote the growth of PLLA attached to their surface.[23,24] Figure 1(b) shows the form of talc is lamellar with a few microns in size.[19] For the sake of brevity, only SEM analyses of PLLA-0.2-4.7 and PLLA-0.2-16.7 are shown because all the composites show a good dispersion. Note that there are obvious orientations of talc lamellae in the direction of melt flow at high talc content.

Crystallization and Melting Behavior

The non-isothermal crystallization and melting behavior of the PLLA/BSAD/talc composites are investigated by DSC. Figure 2 presents the cooling curves of neat PLLA and PLLA/BSAD/talc composites. Comparing to the small, even disappeared crystallization peak of PLLA, the crystallization peak of PLLA with BSAD/talc system is significantly higher and sharper upon cooling. Besides, adding talc shifts the crystallization peak to a higher temperature (around 130°C) than that by adding just BSAD or talc. This result demonstrates that the synergistic effect of BSAD/talc as nucleating agent on increasing crystallization rate is more dramatic than that of single BSAD or talc during cooling. At an elevated temperature, the crystallization of PLLA could be induced by the micro talc particles as preformed nuclei without waiting for BSAD precipitating from the system.

As the content of talc is increased up to 16.7 wt %, however, the crystallization peak has no obvious change or even moves to a lower temperature. It is explained that the crystallization is limited by the poorer chain mobility of PLLA associated with lower T_g rather than the nucleation rate at high temperature upon cooling.[3] The presence of intercalated-structure at high

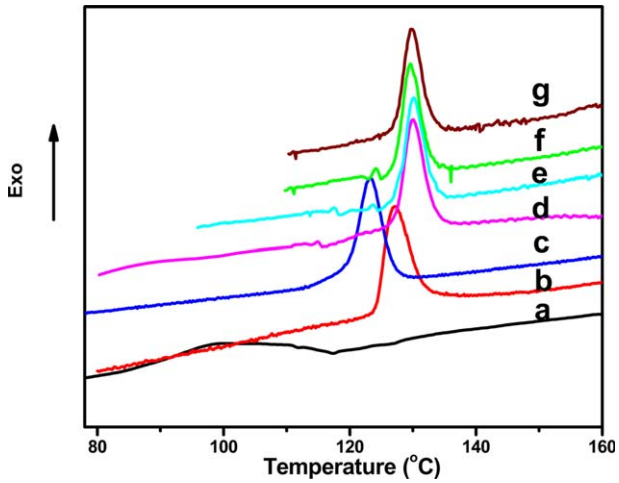

Figure 2. DSC cooling curves of PLLA and PLLA /BSAD/talc composites: (a) pure PLLA, (b) PLLA-0–4.7, (c) PLLA-0.2-0, (d) PLLA-0.2-4.7, (e) PLLA-0.2-9.0, (f) PLLA-0.2-13.0, and (g) PLLA-0.2-16.7. [Color figure can be viewed in the online issue, which is available at wileyonlinelibrary.com.]

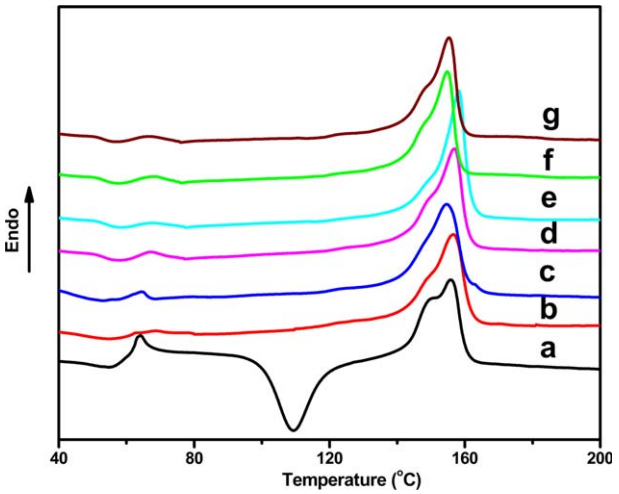

Figure 3. DSC melting curves of PLLA and PLLA/BSAD/talc composites after annealing at 120°C for 5 min: (a) pure PLLA, (b) PLLA-0.2-0, (c) PLLA-0.2-4.7, (d) PLLA-0.2-9.0, (e) PLLA-0.2-13.0, (f) PLLA-0.2-16.7, and (g) PLLA-0.2-16.7. [Color figure can be viewed in the online issue, which is available at wileyonlinelibrary.com.]

talc loading [Figure 1(d)] reduces the PLLA chain mobility. This reduction negatively affects the crystallization process.

The DSC melting curves of samples are described as Figure 3. The obtained calorimetric data are listed in Table I. The incorporation of BSAD/talc in PLLA results in no significant changes in the T_g (around 63°C) upon melting. It is shown that there is a cold crystallization peaks (around109°C) and two overlapping melting peaks (around 147°C and 155°C) for pure PLLA which correspond to crystal formed in cold crystallization and melting, respectively.[25] However, there are no obvious cold crystallization peaks for PLLA/BSAD/talc composites which indicate that the crystals are more perfect during annealing by adding BSAD/talc. That is to say the heterogeneous nucleation of BSAD/talc system is strong enough to eliminate the secondary crystallization existed in melting upon heating.[25,26] Crystals which come first interlock the chains prevent PLLA from forming more crystals through the cold crystallization process. This situation can also be verified by the almost vanishing of lower temperature shoulder peak in heating curves of PLA/BSAD/talc composites.

It is should be noted that the melting peak temperature of PLLA-0.2-4.7 and PLLA-0.2-9.0 shift upward than others (Table I), which means they have more perfect crystals. The crystallinity of PLLA also increases from 6.0% of pure PLLA to a maximum 42.9% of PLLA-0.2-9.0, and then decreases as the increasing dosage of talc. The decrease of crystallinity was ascribed to the poor chain mobility of PLLA caused by excess talc. This phenomenon suggests that there is a balanced effect for BSAD/talc between hindering the polymer chains and improving nucleation and growth of PLLA crystals. BSAD/talc system (0.2/9.0 wt %) exhibits the best cooperative effect on the crystallization of PLLA by increasing nucleation rate and conserving chain mobility to the greatest extent.

Isothermal Crystallization Kinetics

The isothermal crystallization kinetics of samples can be analyzed using the Avrami equation[27] as following [eq. (2)]:

$$1-X_t=\exp(-kt^n) \tag{2}$$

where X_t is the relative crystallinity at crystallization time t, n is the Avrami exponent that reflects the nucleation mechanism and growth dimension of the crystals and k is the rate constant. The relative crystallinity X_t at time t can be obtained by the ratio of enthalpy determined by DSC using eq. (3):

Table I. Thermal Properties and the Crystallinity of Pure PLLA and PLLA/BSAD/Talc Composites

Samples	T_g (°C)	T_m (°C)	T_c (°C)	ΔH_m (J/g)	X_c (%)
PLLA	62.1	155.9	-	34.2 ± 0.1	6.0 ± 0.1
PLLA-0-4.7	62.1	156.7	127.3	32.2 ± 0.5	36.1 ± 0.6
PLLA-0.2-0	61.6	154.7	123.3	36.6 ± 0.5	39.1 ± 0.5
PLLA-0.2-4.7	64.0	156.9	130.1	35.8 ± 0.6	40.2 ± 0.7
PLLA-0.2-9.0	63.0	158.3	130.1	36.5 ± 0.5	42.9 ± 0.6
PLLA-0.2-13.0	62.3	154.8	129.7	32.1 ± 0.4	39.5 ± 0.5
PLLA-0.2-16.7	63.3	155.4	129.8	30.5 ± 0.2	39.3 ± 0.3

T_c, crystallization temperature of cooling; T_m, melt temperature of heating; ΔH_m, melt exotherm of heating.

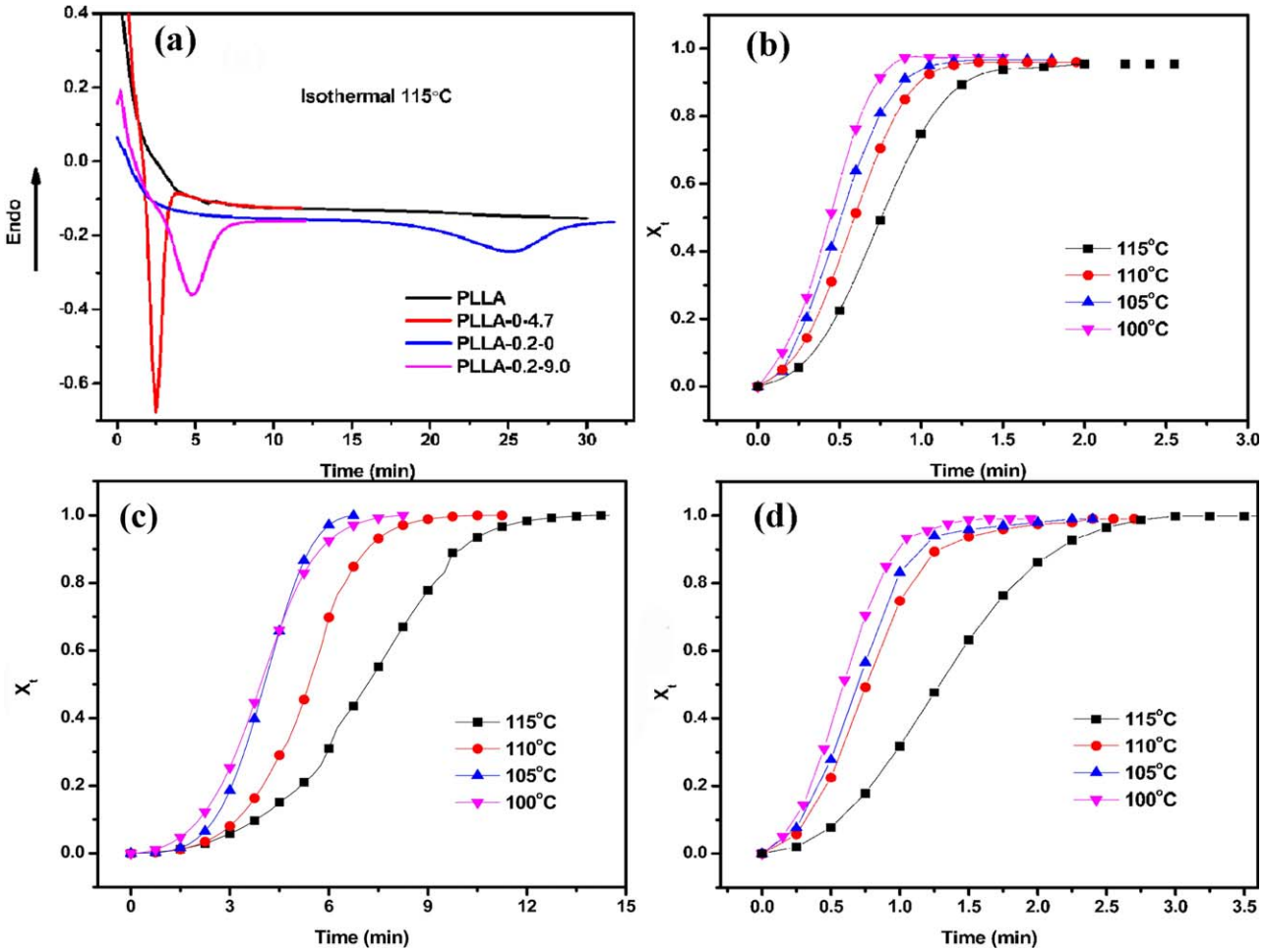

Figure 4. (a) DSC curves of samples isothermally crystallized at 115°C; the crystallinity of composites (b) PLLA-4.7-0, (c) PLLA-0.2-0, and (d) PLLA-0.2-9.0 at different times in isothermal crystallization for different temperatures. [Color figure can be viewed in the online issue, which is available at wileyonlinelibrary.com.]

$$X_t = \frac{\int_0^t \left(\frac{dH_c}{dt}\right) dt}{\int_0^\infty \left(\frac{dH_c}{dt}\right) dt} \tag{3}$$

Taking the double logarithm of eq. (2) gives eq. (4):

$$\ln[-\ln(1-X_t)] = \ln k + n \ln t \tag{4}$$

The plot of $\ln[-\ln(1-X_t)]$ as a function of $\ln(t)$ should be linear. The crystallization rate constant k and Avrami exponent n in the Avrami equation can be determined, respectively, from the intercept and slope of the linear fit portion. On the other hand, the crystallization rate can be estimated by determining the crystallization half-time ($t_{1/2}$).

$$t_{1/2} = (\ln 2/k)^{1/n} \tag{5}$$

Figure 4 describes DSC curves of samples (a) isothermally crystallized at 115°C and the crystallinity at different times in isothermal crystallization for PLLA composites: (b) PLLA-4.7-0, (c) PLLA-0.2-0, and (d) PLLA-0.2-9.0. As can be seen in Figure 4(a) where there was no peak in the process of isothermal crystallization for pure PLLA, it is impossible to do the calculation. It is mainly attributed to the poor crystallization ability of pure PLLA. The crystallization rate constant k, Avrami exponent n, and the reciprocal crystallization half-time obtained from all isothermal crystallizations at 100, 105, 110, and 115°C for PLLA composites are listed in Table II. To our best knowledge, the value of the Avrami exponent n is very near to 3 for pure PLLA isothermally crystallized, implying a three-dimensional heterogeneous crystal growth mechanism.[28] n of PLLA-0.2-0 composite is about 3.0, deducing the mechanism of nucleation and growth of the crystal is not changed. However that of PLLA-0-4.7 composite is all about 2.0, thus the mechanism of nucleation and growth of the crystal is changed and become more similar to a two-dimensional growth on a lamellar structure, which has been reported in the literature.[19] The temperature dependence of $1/t_{1/2}$ of PLLA composites decreases with increasing crystallization temperature (T_c).

The secondary nucleation theory of Lauritzen and Hoffman et al.[29,30] is used to analyze the crystal growth kinetics of PLLA and its composites:

$$\mathrm{G(T)} = G_0 \exp\left(\frac{-U^*}{R(T_C - T_\infty)}\right) \exp\left(\frac{-K_g}{T_C \Delta T f}\right) \tag{6}$$

where G is the spherulite growth rate (G), K_g is the nucleation parameter, T_c is the crystallization temperature, ΔT is the degree

Table II. Avrami Exponent, n, Rate Constant, k (min^{-n}), and Reciprocal Crystallization Half-Time, $1/t_{1/2}$ (min^{-1}), of Pure PLLA and PLLA/BSAD/Talc Composites Isothermally Crystallized at Various Temperatures

	PLLA			PLLA-0-4.7			PLLA-0.2-0			PLLA-0.2-9.0		
T_c (°C)	n	ln(k)	$1/t_{1/2}$	n	ln(k)	$1/t_{1/2}$	n	ln(k)	$1/t_{1/2}$	n	ln (k)	$1/t_{1/2}$
100	-	-	-	1.68	1.05	1.50	2.61	−3.82	0.20	1.90	0.63	1.15
105	-	-	-	1.77	0.69	1.20	3.41	−5.11	0.20	1.83	0.24	0.93
110	-	-	-	1.74	0.48	1.07	3.08	−5.42	0.15	1.84	0.02	0.83
115	-	-	-	1.73	−0.05	0.79	2.65	−5.40	0.11	2.22	−0.90	0.57

of the undercooling expressed as $(T_m^0 - T_c)$, U^* is the activation energy for transport of macromolecular segments to the crystallization site and usually taken as 6280 J/mol,[31] f is the correction factor defined by $2T_C/(T_c + T_m^o)$, R is the gas constant, T_∞ expressed as $T_g - 50$ K is the hypothetical temperature where it can be assumed that all motion associated with viscous flow ceases and G_0 is the front constant.[28]

It has been demonstrated that the results obtained from Lauritzen-Hoffman theory is consistent with that of Avrami theory and the spherulite growth rate (G) is regarded to proportional to $1/t_{1/2}$ ($G = Ck^{1/n}$).[32,33] To determine the K_g, the Lauritzen-Hoffman equation was modified as following:[30,34]

$$\frac{\ln k}{n} + \frac{U^*}{R(T_c - T_\infty)} = \frac{\ln G_0}{C} - \frac{K_g}{T_c f \Delta T} \quad (7)$$

Figure 5 shows the plots of $\frac{\ln k}{n} + \frac{U^*}{R(T_c - T_\infty)}$ versus $10^5/T_c f \Delta T$ and K_g values can be determined by the slopes of the fitted lines. The parameters obtained from the secondary nucleation analysis of PLLA composites are listed in Table III. According to the regime theory, regime I, II, and III are determined by nucleation rate (i) and substrate completion rate (g). As can be seen in Figure 6, PLLA-0-4.7 sample shows crystallization regime III ($i > g$), revealing that talc as nucleating agent mainly increases the nucleation density of PLLA. However, PLLA-0.2-0 sample shows crystallization regime II ($i \sim g$), indicating that BSAD has excellent interfacial adhesion and enhances the segmental mobility of PLLA. The K_g of PLLA-0.2-9.0 (1.14×10^5) is lower that of PLLA-0-4.7 (1.14×10^5), which is ascribed to the reduced chain mobility caused by high content of talc.

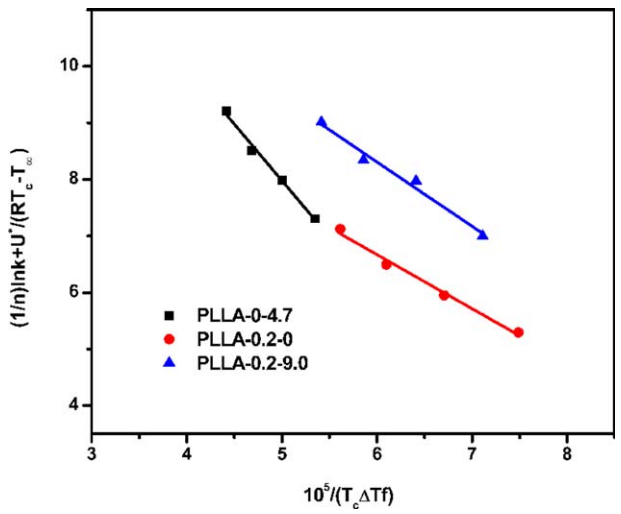

Figure 5. Plots of $\frac{\ln k}{n} + \frac{U^*}{R(T_c - T_\infty)}$ versus $10^5/T_c f \Delta T$ of PLLA/BSAD/talc composites. [Color figure can be viewed in the online issue, which is available at wileyonlinelibrary.com.]

Isothermal Crystallization Morphology

The crystallization morphologies obtained after isothermal crystallization at 120°C for 20 min are shown in Figure 6. Pure PLLA exhibits typical Maltese Cross and regular spherulites with the average diameter of 30–40 μm. Compared with pure PLLA, irregular spherulites with bigger diameters are observed for PLLA-0.2-0 sample. This is ascribed to the plasticizing role of BSAD which enhances the segmental mobility of PLLA and facilitates the growth of spherulites simultaneously.[15] On the other hand, talc as heterogeneous nucleating agent for PLLA crystallization increases the nucleation density of PLLA apparently, and the growth of the crystal is more similar to a two-dimensional growth on a lamellar structure, which has been proved by the analysis of isothermal crystallization kinetics. Compared with PLLA-0-4.7, the similar phenomenon is observed for PLLA-0.2-9.0 with high talc content, but the density of crystal structure becomes bigger because of the presence of BSAD. The synergistic effects of BSAD and talc as nucleating agent on promoting the crystallization of PLLA are by increasing growth of spherulites and nucleation density, respectively. Furthermore, one should notice that some little needle-like crystal appears for PLLA-0.2-0 after isothermal crystallization at 120°C, which can be deduced that the crystalline morphology of PLLA/BSAD is a mixture of spherulite and needle-like crystal.[35]

Heat Deflection Test

As discussed above, the basic idea of incorporating talc into the PLLA/BSAD composites is that talc can provide supplementary nucleation effect to small amount of BSAD, which can increase the heat deflection resistance of PLLA materials. The

Table III. Results of the Secondary Nucleation Analysis and Parameters Used in the Lauritzen–Hoffman Equation

PLLA-BSAD-talc (wt %)	T_g (°C)	T_m^0(°C)	K_g (K^2)
PLLA-0-4.7	62	166	2.00×10^5
PLLA-0.2-0	62	151	0.96×10^5
PLLA-0.2-9.0	63	153	1.14×10^5

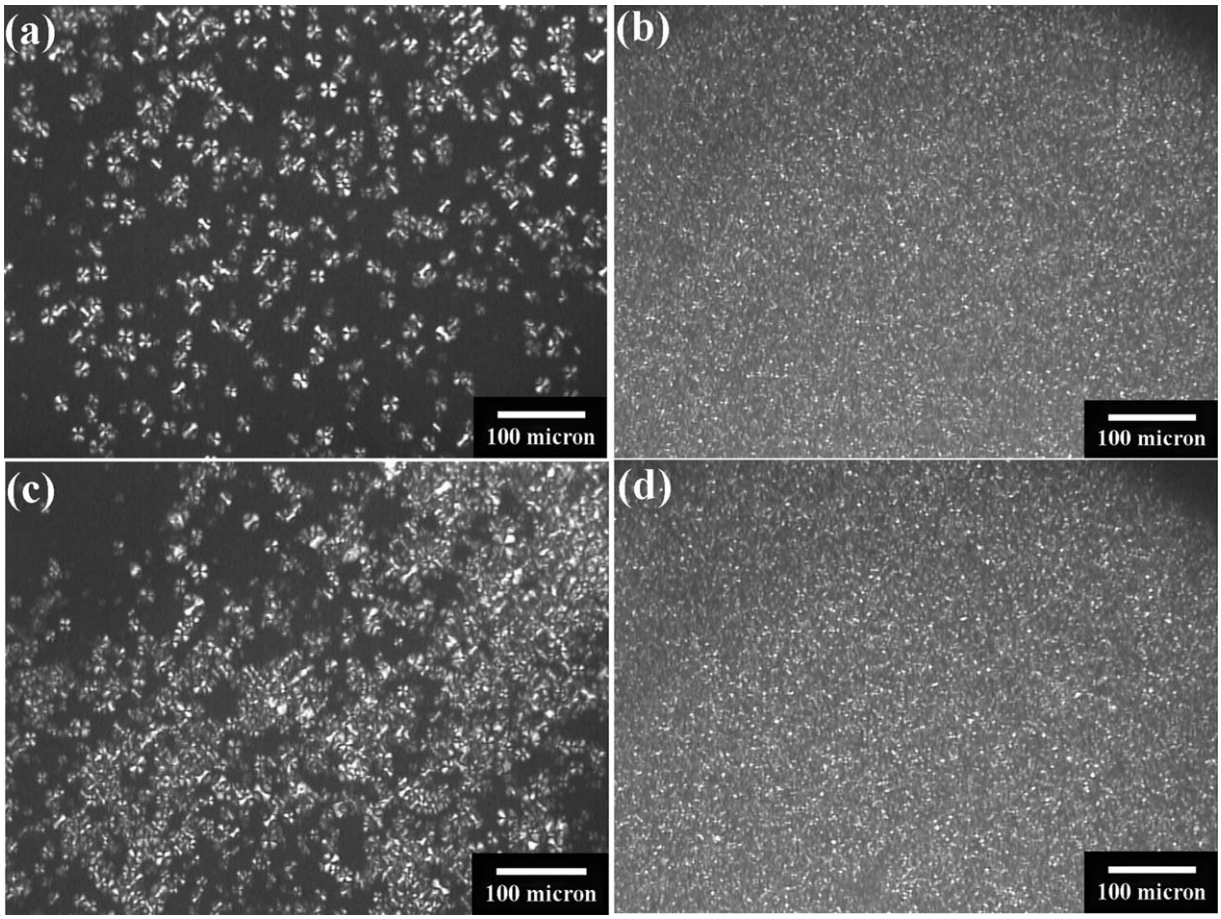

Figure 6. POM images showing the isothermal crystallization morphologies obtained after isothermal crystallization 120°C for 20 min: (a) Pure PLLA, (b) PLLA-0-4.7, (c) PLLA-0.2-0, and (d) PLLA-0.2-9.0.

improvement of HDT is the main purpose in this study. For the practical aim, injection-molding specimens of PLLA composites with different BSAD/talc content are annealed at 120°C, 130°C, and 140°C for 5 min, respectively. To a certain degree, injection-molding specimens are like samples quenched from melt because of high cooling rate. These specimens will experience notable cold crystallization during annealing.

The results of HDT testing are described in Table IV. The HDT of PLLA with only 4.7 wt % talc is improved after annealed, compared with that of pure PLLA. This is ascribed to the effect of talc as crystallization nuclei. It is noted that without adding talc, the HDT of PLLA-0.2-0 decrease from 100.9°C to 80.8°C with increasing the annealing temperature from 120°C to 140°C. It is explained that the crystalline morphology of PLLA/BSAD changes from spherulite to needle-like crystal as reducing the annealing temperature at the early stage of cold crystallization.[35] The crystallization rate of the needle-like crystal is much faster than that of spherulite. Thus BSAD with a minute dosage 0.2 wt % can form fitting needle structure and enhance the crystallization of PLLA only at moderate temperature.

At annealing temperature of 120°C, adding talc can seriously decrease the HDT of composites. This is ascribed to the reduced chain mobility caused by talc. Therefore, adding more talc would produce three dynamic effects, reducing chain mobility, increasing crystallization nuclei and reinforcing polymer matrix by particles. The HDT of PLLA-0.2-4.7 is 63.7°C and increases to 93°C with the talc content 16.7 wt %, which is consistently lower than PLLA with only 0.2 wt % BSAD.

Non-isothermal crystallization tests have proved that BSAD/talc nucleate PLLA at higher temperature than only BSAD. When the annealing temperature was elevated to 130°C or 140°C, it

Table IV. HDT of Pure PLLA and PLLA/BSAD/Talc Composites After Heat Treatment at 120°C, 130°C, and 140°C

	HDT (°C) after heat treatment		
PLLA-BSAD-talc (wt %)	120°C	130°C	140°C
PLLA	56.6	61.0	61.5
PLLA-0-4.7	60.6	81.3	77.0
PLLA-0.2-0	100.9	90.1	80.8
PLLA-0.2-4.7	63.7	95.8	86.2
PLLA-0.2-9.0	73.0	100.7	104.6
PLLA-0.2-13.0	81.1	107.5	107.3
PLLA-0.2-16.7	93.0	110.2	114.6

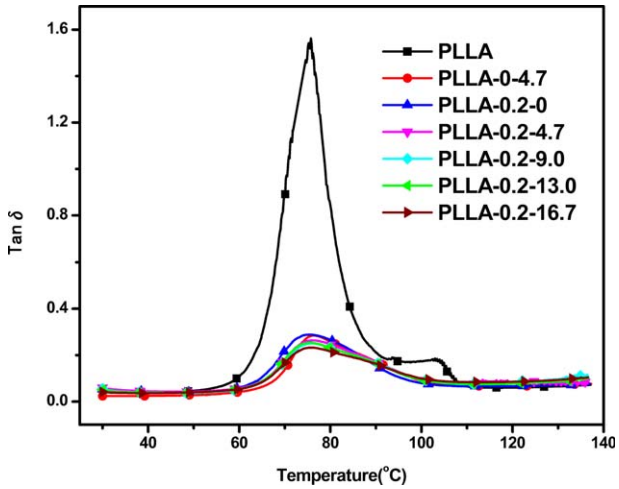

Figure 7. Tan δ versus temperature of PLLA and PLLA/BSAD/talc composites. [Color figure can be viewed in the online issue, which is available at wileyonlinelibrary.com.]

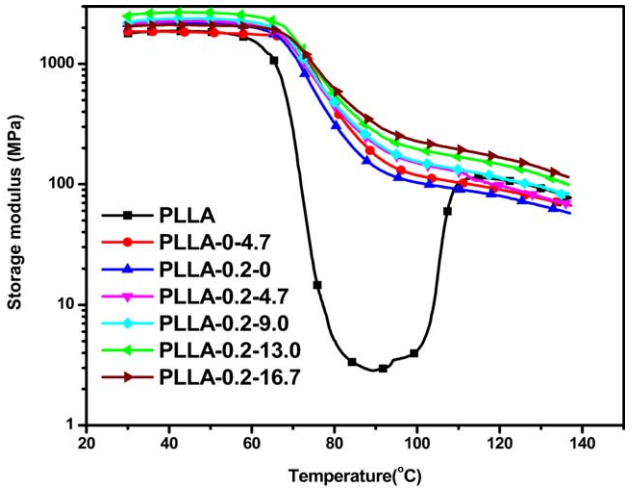

Figure 8. Storage modulus (E') versus temperature of PLLA and PLLA/BSAD/talc composites. [Color figure can be viewed in the online issue, which is available at wileyonlinelibrary.com.]

will weaken the hindrance to chain movement imposed by talc particle and benefit talc for working as nucleation agent. The final HDT of composites are resulted from a combination effect between restricted chain movement and acceleration of crystallization. As we can see from Table II, with talc content over 9.0 wt % and treating temperature over 130°C, the shortcomings of lacking BSAD nuclei and restricted chain movement are fully compensated by reinforcement and acceleration of crystallization process. This leads to an obvious improvement of HDT of PLLA composite. Even though 0.2 wt % BSAD with 9.0 wt % talc exhibit the best effect on crystallization of PLLA, PLLA-0.2-16.7 treated at 140°C show the highest HDT of 114.6°C. It demonstrated higher annealing temperature makes more crystals for composites with high talc content and the reinforcement of talc particles plays an important role on the mechanical properties of PLLA composites at high temperature. The improvement of HDT is due to the effect of talc added and the presence of crystal. Further interpretations about this synergistic effect of BSAD and talc on mechanical behavior of PLLA are done by DMA test.

Dynamic Mechanical Properties

Because of easy deformation of injection-molding PLLA specimens at high temperature, all tested specimens are annealed at 120°C for 5 min before testing. Figures 7 and 8 report tan δ and storage modulus (E') of pure PLLA and PLLA composites, respectively. As the temperature increases, there is a dramatic drop of E' for pure PLLA due to the movement of molecular segments (onset temperature around 60°C). Then the curves of E' rise up again with the temperature up to around 90°C. It demonstrates that pure PLLA still exhibits obvious glass transition and cold crystallization after annealing.

Under glass transition temperature, the addition of talc and BSAD leads to no relevant differences in the storage modulus. Thus the main reinforcing effect in this case is due to the glassy state of PLLA. Significant improvement of storage modulus E' is observed over the glass transition temperature (around 65°C) upon adding BSAD and talc. The storage modulus E' of PLLA containing BSAD, talc and BSAD/talc drops gently to a fixed value and does not show rise caused by cold crystallization. This suggests the main reinforcement effect at high temperature is ascribed to the crystallization induced by BSAD and talc on the PLA during annealing process. At high temperature, the addition of talc leads to a gradual increase of storage modulus. At 110°C the storage modulus increases from 96 MPa for PLLA-0.2-0 to 105 MPa, 142 MPa, 181 MPa, and 207 MPa with the BSAD/talc content 0.2/4.7 wt %, 0.2/9.0 wt %, 0.2/13.0 wt %, and 0.2/16.7 wt %, respectively. It can be seen from Figure 9 that the increasing of the storage modulus is in linear to talc concentration above 4.7 wt % content.

These facts suggest that the thermo-mechanical properties of PLLA is mainly determined by the crystallinity over the T_g and also increases as the talc content of BSAD/talc increase because of the reinforcement effect of talc particles in the polymer matrix. The rigidity of PLLA composites at high temperature, in

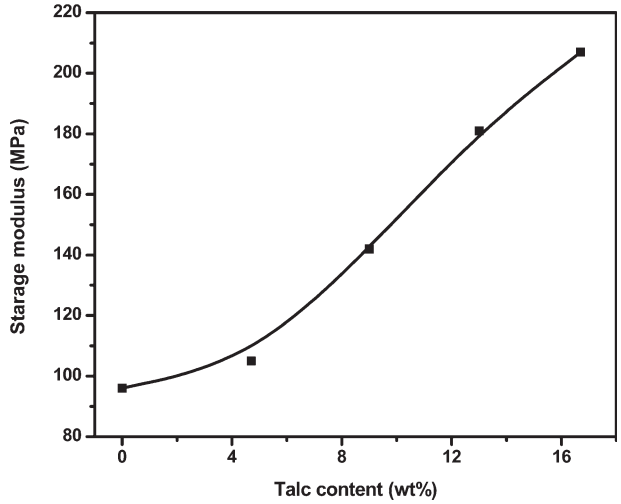

Figure 9. Storage modulus of PLLA/BSAD and PLA/BSAD/talc composites at 110°C.

Table V. Mechanical Properties of PLLA and PLLA/BSAD/Talc Composites

PLLA-BSAD-talc (wt %)	Young's modulus (MPa)	Tensile strength (MPa)	Notched impact strength (KJ/m^2)	Elongation at break (%)
PLLA	2031.2 ± 298.3	77.4 ± 1.6	2.2 ± 0.1	6.4 ± 0.8
PLLA-0-4.7	2627.3 ± 94.7	73.9 ± 1.8	4.4 ± 0.1	4.7 ± 0.3
PLLA-0.2-0	2284.4 ± 204.0	81.4 ± 1.3	2.6 ± 0.1	8.9 ± 0.8
PLLA-0.2-4.7	2555.5 ± 95.2	70.6 ± 1.0	4.5 ± 0.1	4.3 ± 0.2
PLLA-0.2-9.0	2872.8 ± 67.5	69.1 ± 1.3	3.8 ± 0.2	4.3 ± 0.2
PLLA-0.2-13.0	3110.7 ± 110.9	64.2 ± 1.6	3.1 ± 0.1	4.0 ± 0.1
PLLA-0.2-16.7	3625.3 ± 69.6	61.1 ± 0.1	2.4 ± 0.1	3.9 ± 0.2

other words, heat deflection resistance is given by linear addition of talc effect and crystal presence. Provided the composites meet criteria of processing and application, adding as much talc as possible will be conductive to develop PLLA composite with high deflection temperature.

Mechanical Properties

The Young's modulus, elongation at break, tensile and notched impact strength of pure PLLA and its composites are showed in Table V and Figure 10. The Young's modulus of PLLA/BSAD/talc composites is improved and increases with increasing talc content. Compared with the modulus of pure PLLA (2031.2 MPa), that of PLLA-0.2-16.7 (3625.3 MPa) significantly increases by 78.5%, which may be attributed to the reinforcement of talc. On the other hand, the elongation to break is affected by the volume fraction of the added reinforcement, the dispersion of the reinforcement in the matrix, and the interaction between the reinforcement and the matrix.[1] The elongation at break of PLLA/BSAD/talc is reduced except PLLA-0.2-0. The reason is that interfacial adhesion between PLLA and talc is poor and talc causes substantial local stress concentrations. The elongation at break of PLLA-0.2-0 increases apparently, which is because of the proved fact that excellent interfacial adhesion is formed by hydrogen bonding.[23,24] Pure PLLA presents notched impact strength of 2.2 KJ/m^2. As can be seen from Figure 10(b), adding only BSAD or talc improved notched impact strength to 2.6 KJ/m^2 and 4.4 KJ/m^2, respectively. The notched impact strength of all PLLA composites is enhanced, and that of PLLA-0.2-4.7 reaches a maximum value around 4.5 KJ/m^2. As a result, this strengthening effect is consistent with the crystallinity, which further deduces that the crystalline phase can confer mechanical properties above T_g. Besides, the notched impact strength decreases apparently when the content of talc is 16.7 wt %, which may be attributed to more stress concentration points generated by high content of talc.[36] On the other hand, the tensile strength of pure PLLA is 77.4 MPa. There is a slightly decrease from 81.4 to 61.1 MPa in the tensile strength of PLLABSAD/talc composites with increasing talc content. It is ascribed to the poor adhesion between talc and PLLA.

CONCLUSION

The poor heat resistance caused by low crystallization rate of PLLA was addressed by addition of a nucleating agent system. It is found that BSAD/talc system has synergistic effects on the physical and mechanical behavior of PLLA, especially when 0.2 wt % BSAD and 9.0 wt % talc were added simultaneously.

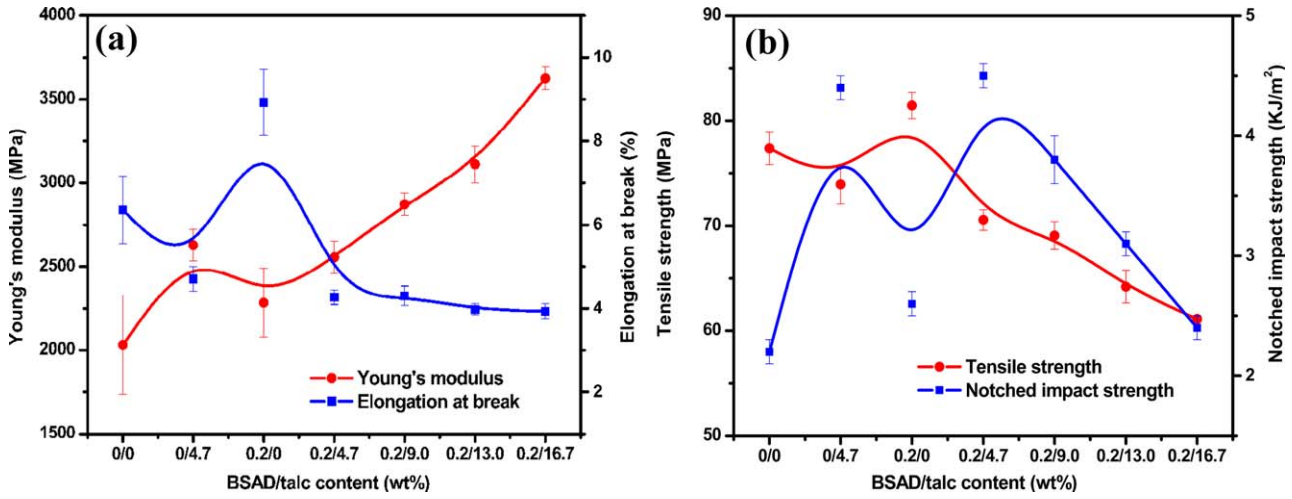

Figure 10. Mechanical properties of PLLA and PLLA/BSAD/talc composites: (a) Young's modulus and Elongation at break and (b) Tensile and notched impact strength. [Color figure can be viewed in the online issue, which is available at wileyonlinelibrary.com.]

The crystallization behavior of PLLA/BSAD/talc composites during cooling is mainly influenced by the nucleation rate and chain mobility. There is a balanced effect for talc between hindering the polymer chains and improving nucleation and growth of PLLA crystals. Upon melting, without the cold crystallization, the crystallinity of PLA/BSAD/talc composites also increases from 6.0% of pure PLLA to a maximum 42.9% at 9.0 wt % of talc. According to the kinetics and morphology of isothermal crystallization, the synergistic effects of BSAD and talc as nucleating agent on promoting the crystallization of PLLA are by increasing the growth of spherulites and nucleation density, respectively. PLLA-0.2-16.7 annealed at 140°C for 5 min shows the highest HDT of 114.6°C. Over the T_g, the storage modulus increase is ascribed to the synergistic effect of BSAD/talc system between crystallinity and reinforcement in the polymer matrix. Moreover, the increases of the storage modulus are in linear to talc concentration over 4.7 wt %, and the notched impact strength of PLLA/BSAD/talc composites was significantly improved.

REFERENCES

1. Pei, A. H.; Zhou Q.; Berglund L. A. *Compos. Sci. Technol.* **2010**, *70*, 815.
2. Celli, A.; Scandola, M. *Polymer* **1992**, *33*, 2699.
3. Li, H.; Huneault, M. A. *Polymer* **2007**, *48*, 6855.
4. Mitomo, H.; Kaneda, A.; Quynha, T. M.; Nagasawa, N.; Yoshii, F. *Polymer* **2005**, *46*, 4695.
5. Fiore, G. L.; Jing, F.; Young, V. G. Jr.; Cramer, C. J.; Hillmyer, M. A. *Polym. Chem.* **2010**, *1*, 870.
6. Suhartini, M.; Mitomo, H.; Nagasawa, N.; Yoshii, F.; Kume, T. *J. Appl. Polym. Sci.* **2003**, *88*, 2238.
7. Quynh, T. M.; Mitomo, H.; Nagasawa, N.; Wada, Y.; Yoshii, F.; Tamada, M. *Eur. Polym. J.* **2007**, *43*, 1779.
8. Yang, S. L.; Wu, Z. H.; Yang, W.; Yang, M. B. *Polym. Test.* **2008**, *27*, 957.
9. Brochu, S.; Prud'homme, R. E.; Barakat, I.; Jerome, R. *Macromolecules* **1995**, *28*, 5230.
10. Yamane, H.; Sasai, K. *Polymer* **2003**, *44*, 2569.
11. Schmidt, S. C.; Hillmyer, M. A. *J. Polym. Sci., Part B: Polym. Phys.* **2001**, *39*, 300.
12. Huda, M. S.; Drzal, L. T.; Misra, M.; Mohanty, A. K. *J. Appl. Polym. Sci.* **2006**, *102*, 4856.
13. Suryanegara, L.; Nakagaito, A. N.; Yano, H. *Compos. Sci. Technol.* **2009**, *69*, 1187.
14. Xu, J. Z.; Chen, T.; Yang, C. L.; Li, Z. M.; Mao, Y. M.; Zeng, B. Q.; Hsiao, B. S. *Macromolecules* **2010**, *43*, 5000.
15. Li, Y. L.; Wu, H. Y.; Wang, Y.; Liu, L.; Han, L.; Wu, J.; Xiang, F. M. *J. Polym. Sci., Part B: Polym. Phys.* **2010**, *48*, 520.
16. Kawamoto, N.; Sakai, A.; Horikoshi, T.; Urushihara, T.; Tobita, E. *J. Appl. Polym. Sci.* **2007**, *103*, 244.
17. Kawamoto, N.; Sakai, A.; Horikoshi, T.; Urushihara, T.; Tobita, E. *J. Appl. Polym. Sci.* **2007**, *103*, 198.
18. Haubruge, H. G.; Daussin, R.; Jonas, A. M.; Legras, R. *Macromolecules* **2003**, *36*, 4452.
19. Battegazzore, D.; Bocchini, S.; Frache, A. *eXPRESS Polym. Lett.* **2011**, *5*, 849.
20. Ke, T.; Sun, X. *J. Appl. Polym. Sci.* **2003**, *89*, 1203.
21. Nam, J. Y.; Ray, S. S.; Okamoto, M. *Macromolecules* **2003**, *36*, 7126.
22. Saeidlou, S.; Huneault, M. A.; Li, H. B.; Park, C. B. *Prog. Polym. Sci.* **2012**, *37*, 1657.
23. Zhou, S. B.; Zheng, X. T.; Yu, X. J.; Wang, J. X.; Weng, J.; Li, X. H.; Feng, B.; Yin, M. *Chem. Mater.* **2007**, *19*, 247.
24. Cai, Y.; Yan, S.; Yin, J.; Fan, Y.; Chen, X. *J. Appl. Polym. Sci.* **2011**, *121*, 1408.
25. Tábi, T.; Sajó, I. E.; Szabó, F.; Luyt, A. S.; Kovács, J. G. *Exp. Polym. Lett.* **2010**, *4*, 659.
26. Huang, S. M.; Hwang, J. J.; Liu, H. J.; Lin, L. H. *J. Appl. Polym. Sci.* **2010**, *117*, 434.
27. Li, J.; Fang, Z.; Zhu, Y.; Tong, L.; Gu, A.; Liu, F. *J. Appl. Polym. Sci.* **2007**, *105*, 3531.
28. Miyata, T.; Masuko, T. *Polymer* **1998**, *39*, 5515.
29. Tsuji, H.; Wada, T.; Sakamoto, Y.; Sugiura, Y. *Polymer* **2010**, *51*, 4937.
30. Lauritzen, J. I., Jr.; Hoffman, J. D. *J. Appl. Phys.* **1973**, *44*, 4310.
31. Shieh, Y. T.; Twu, Y. K.; Su, C. C.; Lin, R. H.; Liu, G. L. *J. Polym. Sci., Part B: Polym. Phys.* **2010**, *48*, 983.
32. Liang, G. D.; Qin, W. P.; Liu, T. T.; Zhu, F. M.; Wu, Q. *J. Appl. Polym. Sci.* **2012**, *125*, E113.
33. Lannace, S.; Nicolais, L. *J. Appl. Polym. Sci.* **1997**, *64*, 911.
34. Hoffman, J. D.; Weeks, J. J. *J. Chem. Phys.* **1962**, *37*, 1723.
35. Takahashi, K.; Sugimoto, M.; Taniguchi, T.; Koyama, K. 5th Pacific Rim Conference on Rheology, Hokkaido, Japan, Aug 1–6, 2010.
36. Petchwattana, N.; Covavisaruch, S.; Petthai, S. *Polym. Bull.* **2014**, *71*, 1947.